A study of dynamic characteristics and simulation of MEMS torsional micromirrors

Jian Ping Zhao[a] *,·Hua Ling Chen , Jian Ming Huang[b], Ai Qun Liu[b]

Institute of Vibration and Noise Control, School of Mechanical Engineering, Xi'an Jiaotong University, Xi'an, Shaanxi 710049, China
School of Electrical & Electronic Engineering, Nanyang Technological University, 50 Nanyang Avenue, Singapore 639798, Singapore

Abstract

The influence of van der Waals (vdW) force on the stability of electrostatic torsional nano-electro-mechanical systems (NEMS) actuators is analyzed in the paper. The dependence of the critical tilting angle and voltage is investigated on the sizes of structure with the consideration of vdW effects. The pull-in phenomenon without the electrostatic torque is studied, and a critical pull-in gap is derived. A dimensionless equation of motion is presented, and the qualitative analysis of it shows that the equilibrium points of the corresponding autonomous system include center points, stable focus points, and unstable saddle points. The Hopf bifurcation points and fork bifurcation points also exist in the system. The phase portraits connecting these equilibrium points exhibit periodic orbits, heteroclinic orbits, as well as homoclinic orbits.

1. INTRODUCTION

The technology of MEMS devices has experienced a lot of progress recently. Their low manufacturing cost, batch production, light weight, small size, durability, low energy consumption, and compatibility with integrated circuits, makes them extremely attractive (Maluf and Williams 1999; Younis 2004). Successful MEMS devices rely not only on well developed fabrication technologies, but also on the knowledge of device behavior, based on which a favorable structure of the device can be forged (Chao et al. 2006). The important role of MEMS devices in optical systems initiate the development of a new class of MEMS called MicroOptoElectro-Mechanical Systems (MOEMS). MOEMS mainly include micromirrors and

NOMENCLATURE

A_{wet}	wet area of the plate	U	potential strain energy of the torsion beams
c	speed of light		
F_{cap}	capillary force	U_{tot}	interfacial energy
F_{Cas}	Casimir force	V	potential energy of applied loads
G	shear modulus of elasticity of the beam's material	W	width of mirror
		W_e	work done by external forces
h	initial distance between the mirror and the substrate	**Greek Letters**	
		γ	surface energy of the liquid
I_p	momentum of inertia of the beams cross section	γ_{LA}	liquid-air interfacial tensions
		γ_{SA}	solid -air interfacial tensions
l	length of each torsion beam	γ_{SL}	solid-liquid interfacial tensions
L	length of mirror	$\prod$	total potential energy of the system
P_{cap}	capillary pressure		
r	width of the torsion beams cross section	θ	tilting angle of the mirror
		θ_c	contact angle
s	length of the torsion beams cross section	Θ	dimensionless tilting angle of the mirror

torsional micro-actuators. These devices have found a variety of applications such as digital micromirror devices (DMD) (Hornbeck 1991), optical switches (Ford et al. 1999), micro scanning mirrors (Bai et al. 2007; Dickensheets and Kino 1998), optical cross connects (Zavracky et al. 1997), and etc.

The existence of a liquid bridge between two objects results in the forming of capillary force (Wei and Zhao 2007). The existence of capillary force even in low relative humidity is observed experimentally (Zwol et al. 2008). Parallel plate MEMS actuators are conventionally fabricated by forming a layer of a plate or beam material on the top of a sacrificial layer of another material and wet etching the sacrificial layer. In this process, capillary force can be easily formed and in the case of poor design, the structure will collapse and adhere to the substrate. So investigating the effect of capillary force on micromirrors is extremely important in their design and fabrication.

Many researchers investigated the effect of capillary force on MEMS devices. Mastrangelo and Hsu (1993) studied the stability and adhesion of thin micromechanical structures under capillary force, theoretically and experimentally. Moeenfard et al. (2010) studied the effect of capillary force on the static pull-in instability of fully clamped micromirrors. The effects of capillary force on the static and dynamic behaviors of atomic force microscopes (AFM) are widely assessed (Zitzler et al. 2002; Li and Peng 2006; Jang et al. 2004). Recently, the instability of torsional MEMS/NEMS micro-actuators under capillary force was investigated by Guo et al. (2009).

When the size of a structure is sufficiently small, Casimir and van der Waals forces play an important role and in the case of poor design, can lead to the collapse of the structure. VdW force is the interaction force between neutral atoms and it differs from covalent and ionic bondings in that it is caused by correlations in the fluctuating polarizations of nearby particles (Xie 2009). Casimir force is understood as the longer distances range analog of the vdW force, resulting from the propagation

of retarded electromagnetic waves, whose distance ranges from a few nanometers up to a few micrometers (Gusso and Delben 2007). An important feature of the Casimir effect is that even though it is quantum in nature, it predicts a force between macroscopic bodies (Bordag et al. 2001). This makes the Casimir force relevant in N/MEMS (Zhao et al. 2003).

Zhao et al. (2003) discussed the Casimir force induced adhesion in MEMS. Tahami et al. (2009) discussed Pull-in Phenomena and Dynamic Response of a Capacitive Nano-beam Switch by considering Casimir effect. Casimir effect on the pull-in parameters of nanometer switches has been studied by Lin and Zhao (2005a). They (Lin and Zhao 2005b) also studied Nonlinear behavior of nano-scale electrostatic actuators with Casimir force. Ramezani et al. (2007; 2008) investigated the two point boundary value problem of the deflection of nano-cantilever subjected to Casimir and electrostatic forces using analytical and numerical methods to obtain the instability point of the nanobeam. Modeling and simulation of electrostatically actuated nano-switches under the effect of Casimir forces have been studied by Mojahedi et al. (2009). Sirvent et al. (2009) theoretically studied pull-in control in capacitive microswitches actuated by Casimir forces using external magnetic fields. Effect of the Casimir force on the static deflection and stiction of membrane strips in MEMS have been studied by Serry et al. (1998). Guo and Zhao (2004) discussed the effect of Casimir force on the pull-in of electrostatic torsional actuators. But statical behavior and pull-in of single sided nano/micromirrors under effect of capillary and Casimir forces has not been investigated. So in this article, the combined effect of Casimir and capillary forces on the tilting angle and stability of torsional nano/micromirror is studied. In this study, HPM is used as a perturbational based analytical tool.

Perturbation methods have been used to analytically solve the nonlinear problems in MEMS. Younis and Nayfeh (2003) investigate the response of a resonant microbeam to an electric actuation using the multiple-scale perturbation method. Abdel-Rahman and Nayfeh (2003) used the same method to model secondary resonances in electrically actuated microbeams. Since perturbation methods are based upon the assumption that there is a small parameter in the equations, they have some limitations in problems without involvement of small parameters. In order to overcome this limitation a new perturbational based method, namely Homotopy Perturbation Method (HPM) was developed by He (2000). His new method takes full advantages of the traditional perturbation methods and homotopy technique. Homotopy perturbation method has also been used for solving the nonlinear problems encountered in N/MEMS. For example, Moeenfard et al. (2011) used HPM to model the nonlinear vibrational behavior of Timoshenko micobeams. Mojahedi et al. (2010) applied the HPM method to simulate the static response of nano-switches to electrostatic actuation and intermolecular surface forces. But so far no analytic solution has been presented to model the behavior of nano/micromirrors.

In the current article, the equations governing the static behavior of rectangular nano/micromirrors are obtained using the minimum potential energy principle. Then pull-in parameters of nano/micromirrors under the effect of Casimir and capillary forces are investigated. At the end, the tilting angle of a nano/micromirror under Casimir and capillary forces is calculated both numerically and analytically using HPM.

2. THEORETICAL MODEL

The contact angle θ_c for a liquid drop shown in Figure 1a is determined by the balance among the liquid-air (LA), solid–air (SA), and solid-liquid (SL) interfacial tensions, which are denoted by γ_{LA}, γ_{SA} and γ_{SL}, respectively (Guo et al. 2009). At the equilibrium state, Young's equation (Knospe and Nezamoddini 2009) is satisfied as follows.

$$\gamma_{SA} = \gamma_{SL} + \gamma_{LA} \cos \theta_c \tag{1}$$

At the equilibrium state, the energy of the system shown in Figure 1b is (Fortes 1982):

$$U_{tot} = 2A_{wet}(\gamma_{SL} - \gamma_{SA}) + C = -2A_{wet}\gamma \cos \theta_c + C \tag{2}$$

where U_{tot} is the interfacial energy, A_{wet} is the wet area of the plate, C is a constant and $\gamma = \gamma_{LA}$ is the surface energy of the liquid. Since the volume of the liquid shown in Figure 1b, $v = zA_{wet}$ is constant, it can be easily concluded that:

$$\frac{dA_{wet}}{dz} = -\frac{A_{wet}}{z} \tag{3}$$

The capillary force can be obtained from the interfacial energy as follows.

$$F_{cap} = -\frac{dU_{tot}}{dz} = 2\gamma \cos \theta_c \frac{dA_{wet}}{dz} = -2\gamma \cos \theta_c \frac{A_{wet}}{z} \tag{4}$$

As a result, the capillary pressure underneath the plate is

$$p_{cap} = -\frac{F_{cap}}{A_{wet}} = \frac{2\gamma \cos \theta_c}{z} \tag{5}$$

Using the obtained equation for capillary pressure, the capillary force applied to the differential surface element of the micromirror shown in Figure 2 is

$$dF_{cap} = \frac{2\gamma \cos \theta_c}{h - x \sin \theta} W dx \tag{6}$$
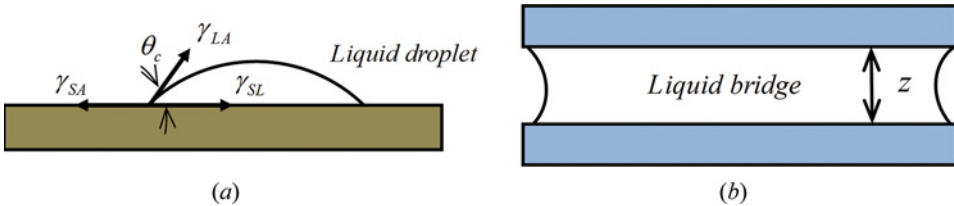

Figure 1. (a) Contact angle of a droplet at a solid-liquid interface (b) Liquid bridge between two parallel plates (color figure available online).
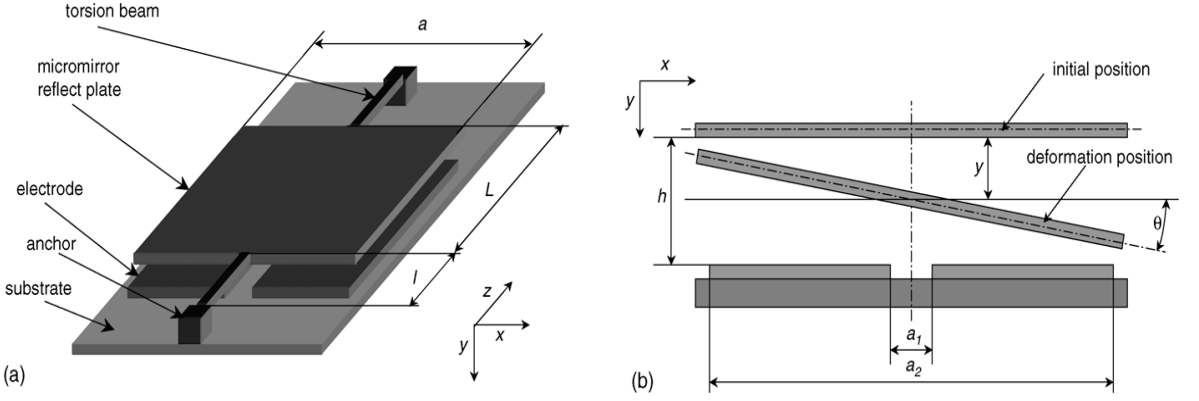
Figure 2. Schematic view of a nano/micromirror (color figure available online).

where h is the initial distance between the mirror and the substrate and θ is the tilting angle of the mirror.

Furthermore the differential Casimir force applied to a differential surface element of the mirror shown in Figure 2 is (Liu et al. 2010):

$$dF_{Cas} = \frac{\pi^2 \hbar c}{240(h - x\sin\theta)^4} \, Wdx \qquad (7)$$

where c is speed of light, $\hbar$ is Plank's constant divided by 2π and W is width of mirror as illustrated in Figure 2.

The minimum total potential energy principle (Rao 2007) is utilized here to obtain equilibrium equation and to investigate the stability of the equilibrium points. The total potential energy of the system can be divided into two parts: the potential strain energy of the torsion beams and the potential energy of applied loads which is equal to the minus of work done by external forces.

$$\prod = U + V = U - W_e \qquad (8)$$

where $\prod$ is the total potential energy of the system, U is the potential strain energy of the torsion beams, V is the potential energy of applied loads and W_e is the work done by external forces. In equilibrium points, variation of the total potential energy of the system is zero.

$$\delta \prod = \delta U - \delta W_e = 0 \qquad (9)$$

The potential strain energy of system can be calculated as:

$$U = \frac{1}{2}K\theta^2 \tag{10}$$

where (Huang 2004)

$$K = \frac{2GI_p}{l} \tag{11}$$

In this equation, G is the shear modulus of elasticity of the beam's material, l is length of each torsion beam and I_p is the polar momentum of inertia of the beams cross section which can be calculated using equation (12) (Huang 2004).

$$I_p = \frac{1}{3}rs^3 - \frac{64}{\pi^5}s^4 \sum_{n=1}^{\infty} \frac{1}{(2n-1)^5} \tanh \frac{(2n-1)\pi r}{2s} \tag{12}$$

where r and s are the width and length of the torsion beams cross section respectively as illustrated in Figure 2.

The variation of U would be as

$$\delta U = K\theta\delta\theta \tag{13}$$

The total external work done on nano/micromirror to rotate it from angle θ to angle $\theta + \delta\theta$ can be calculated as follows.

$$\delta W_e = \int_0^L (dF_{Cap} + dF_{Cas})(x\delta\theta)$$
$$= \int_0^L \left(\frac{2\gamma \cos \theta_c}{h - x\sin\theta} W dx + \frac{\pi^2 \hbar c}{240(h - x\sin\theta)^4} W dx \right)(x\delta\theta) \tag{14}$$

where L is length of mirror as illustrated in Figure 2. Since $\frac{h}{L} \ll 1$, the tilting angle is small, and $\sin\theta$ can be closely approximated by θ. For simplification purpose, the following dimensionless variable is introduced.

$$\Theta = \frac{\theta}{\theta_0} \tag{15}$$

where $\theta_0 \approx \sin\theta_0 = \frac{h}{L}$ is the maximum physically possible rotation angle of the mirror.

At equilibrium points, equation (9) must be satisfied. So by performing the integration in equation (14), the equilibrium equation is obtained as follows.

$$\frac{\eta}{\Theta}\left(1 + \frac{1}{\Theta}\ln(1-\Theta)\right) - \frac{\lambda}{\Theta^2}\left(\frac{1}{6} - \frac{3\Theta-1}{6(\Theta-1)^3}\right) + \Theta = 0 \tag{16}$$

where η and λ are called instability numbers and are defined as equations (17) and (18) respectively.

$$\eta = \frac{2\gamma \cos\theta_c \, WL^3}{Kh^2} \tag{17}$$

$$\lambda = \frac{\pi^2 \hbar c \, WL^3}{240 h^5 K} \tag{18}$$

Performing the second variation operator on equation (8) and using equilibrium equation yields:

$$
\delta^2 \prod = \frac{(\delta\Theta)^2 h^2 K}{L^2} \left[1 - \frac{\eta}{\Theta^2}\left(1 + \frac{2\ln(1-\Theta)}{\Theta} + \frac{1}{1-\Theta}\right) \right.
$$
$$
\left. + \frac{\lambda}{\Theta^3}\left(\frac{8}{3}\frac{1}{(1-\Theta)^3} - \frac{2}{(1-\Theta)^2} - \frac{1}{(1-\Theta)^4} + \frac{1}{3}\right) \right] \tag{19}
$$

According to minimum total potential energy principle an equilibrium point is stable when $\delta^2\prod > 0$ and is unstable when $\delta^2\prod < 0$ (Gambhir 2004). So the stability condition is reduced to:

$$
I(\eta, \lambda, \Theta) = 1 - \frac{\eta}{\Theta^2}\left(1 + \frac{2\ln(1-\Theta)}{\Theta} + \frac{1}{1-\Theta}\right)
$$
$$
+ \frac{\lambda}{\Theta^3}\left(\frac{8}{3}\frac{1}{(1-\Theta)^3} - \frac{2}{(1-\Theta)^2} - \frac{1}{(1-\Theta)^4} + \frac{1}{3}\right) > 0 \tag{20}
$$

Finding η from equation (16) and substituting it in equation (20) leads to:

$$
I(\lambda, \Theta) = 1 - \frac{\frac{\lambda}{\Theta^3}\left(\frac{1}{6} - \frac{3\Theta-1}{6(\Theta-1)^3}\right) - 1}{1 + \frac{1}{\Theta}\ln(1-\Theta)}\left(1 + \frac{2\ln(1-\Theta)}{\Theta} + \frac{1}{1-\Theta}\right)
$$
$$
+ \frac{\lambda}{\Theta^3}\left(\frac{8}{3}\frac{1}{(1-\Theta)^3} - \frac{2}{(1-\Theta)^2} - \frac{1}{(1-\Theta)^4} + \frac{1}{3}\right) \tag{21}
$$

Figure 3 shows the function $I(\lambda, \Theta)$ versus Θ at some values of λ.

An equilibrium point is stable if $I(\lambda, \Theta) > 0$ and unstable if $I(\lambda, \Theta) < 0$. It is observed that at certain value of Θ called Θ_P, which relates to the pull-in state, $I(\lambda, \Theta)$ becomes zero. When $\Theta < \Theta_P$, $I(\lambda, \Theta)$ would be positive and the resulting equilibrium point is stable and when $\Theta > \Theta_P$, $I(\lambda, \Theta)$ would be negative and the resulting equilibrium point is unstable.

At the pull-in state, in addition to the equilibrium equations, the following equation is also satisfied.
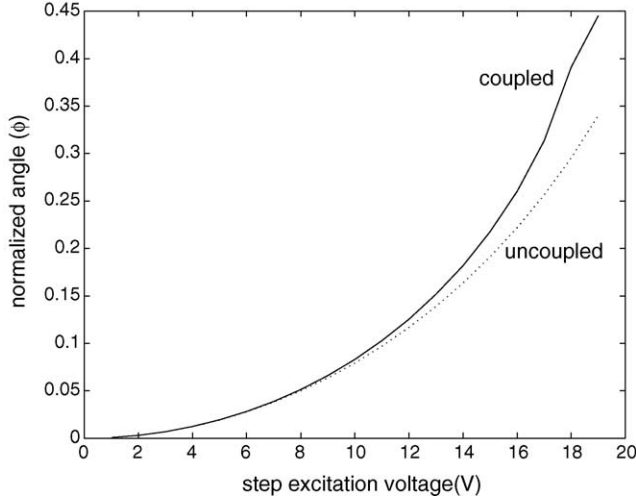
$$I(\eta, \lambda, \Theta) = 0 \tag{22}$$

Figure 3. Function I (λ, Θ) versus Θ (color figure available online).

Equations (16) and (22) can be solved simultaneously for finding η and λ at the pull-in. The results are as follows.

$$\eta_P = -\frac{3\Theta_P^3\left(\Theta_P^2 - 4\Theta_P + 1\right)}{\Theta_P^3 - 3\Theta_P^2 - 6\Theta_P - 6\ln(1 - \Theta_P)} \tag{23}$$

$$\lambda_P = -\frac{6\Theta_P(\Theta_P - 1)^3\left(-\Theta_P^2 + 3(\Theta_P - 1)(\Theta_P + \ln(1 - \Theta_P))\right)}{\Theta_P^3 - 3\Theta_P^2 - 6\Theta_P - 6\ln(1 - \Theta_P)} \tag{24}$$

In equations (23) and (24), λ_P, η_P and Θ_P are the values of λ, η and Θ at pull-in, respectively. Figures 4 and 5 shows the values of pull-in angle versus λ_P and η_P, respectively. It is observed that with increasing the value of λ_P the pull-in angle of the mirror is reduced, while with increasing the η_P, the pull-in angle of the mirror is increased.

By eliminating Θ_P between equations (23) and (24), η_P can be obtained versus λ_P as plotted in Figure 6. It is observed that by increasing the dimensionless Casimir force applied to the mirror λ_P, the mirror resistance to the capillary force is reduced and pull-in occurs at lower values of η. In fact this figure shows that Casimir force can significantly reduce the maximum allowable value for η and as a result, the stability limits of the nano/micromirror are reduced. In addition it can be concluded that even in the absence of capillary force, Casimir force can lead to the occurrence of pull-in. So, in order to have a successful and stable design for nano/micromirrors fabricated using wet etching process where capillary force plays a major role, the inequalities given in equation (25) have to be satisfied.

$$\eta = \frac{2\gamma\cos\theta_c WL^3}{Kh^2} < \eta_p$$
$$\lambda = \frac{\pi^2\hbar c WL^3}{240h^5K} < \lambda_P \tag{25}$$
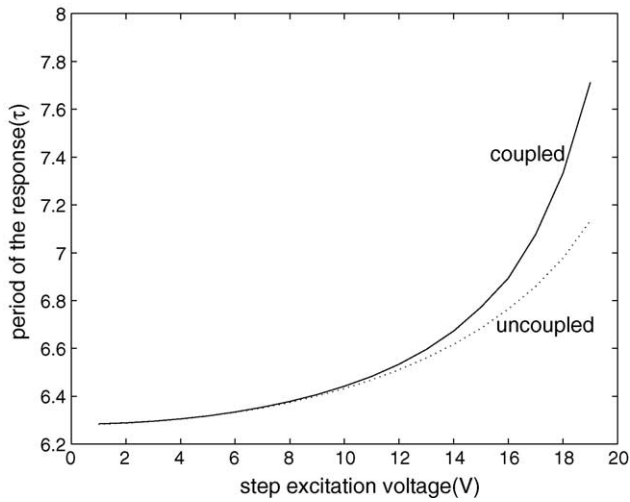
Figure 4. Pull-in angle of mirror versus λ_p (color figure available online).

In order to investigate the mirror's behavior under combined capillary and Casimir loading, the dimensionless rotation angle has been plotted versus η in Figure 7.

It is observed that by increasing the value of η the rotation angle of the nano/ micromirror is increased, but the maximum value of η at pull-in, highly depends on the value of λ and it is verified that by increasing λ, the maximum allowable value for λ is reduced. Furthermore it is concluded that at a constant η, larger values of λ would lead to larger values for stable equilibrium angle.

3. ANALYTICAL SOLUTION OF EQUILIBRIUM EQUATIONS

In this section, we try to find the value of the rotation angle of the nano/micro-mirror analytically in terms of η and λ. For this purpose, the analytical tool, HPM is utilized.
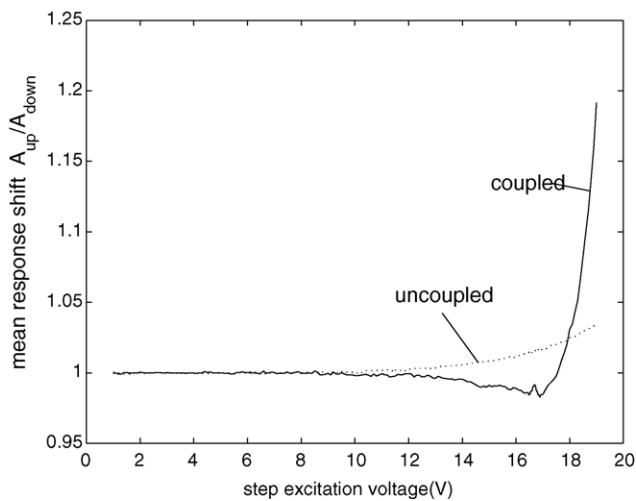

Figure 5. Pull-in angle of mirror versus η_P (color figure available online).

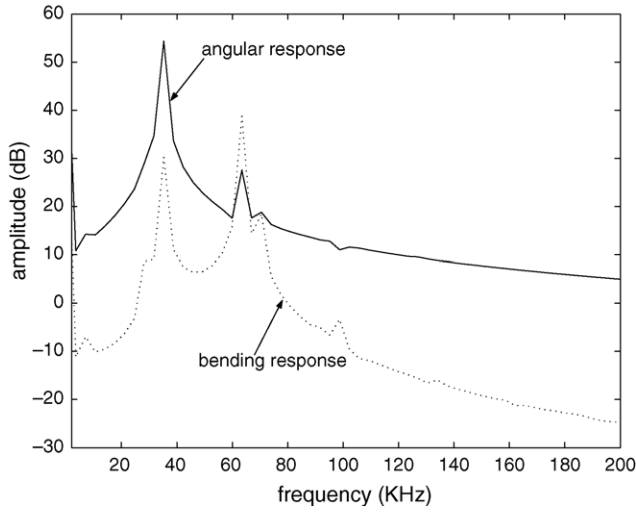Figure 6. η_P versus λ_P (color figure available online).

The linear part of equation (16) can be found by using Taylor series expansion of the equilibrium equation (16) as follows.

$$L(\Theta, \eta, \lambda) = -\frac{\eta + \lambda}{2} + \left(\frac{3 - 4\lambda - \eta}{3}\right)\Theta \qquad (26)$$

where $L(\Theta, \eta, \lambda)$ is the linear part of equation (16). Obviously the nonlinear part of equilibrium equation is obtained by subtracting $L(\Theta, \eta, \lambda)$ from equation (16).

$$N(\Theta, \eta, \lambda) = \frac{\eta}{\Theta}\left(1 + \frac{1}{\Theta}\ln(1 - \Theta)\right) - \frac{\lambda}{\Theta^2}\left(\frac{1}{6} - \frac{3\Theta - 1}{6(\Theta - 1)^3}\right) + \left(\frac{4\lambda + \eta}{3}\right)\Theta + \frac{\eta + \lambda}{2}$$
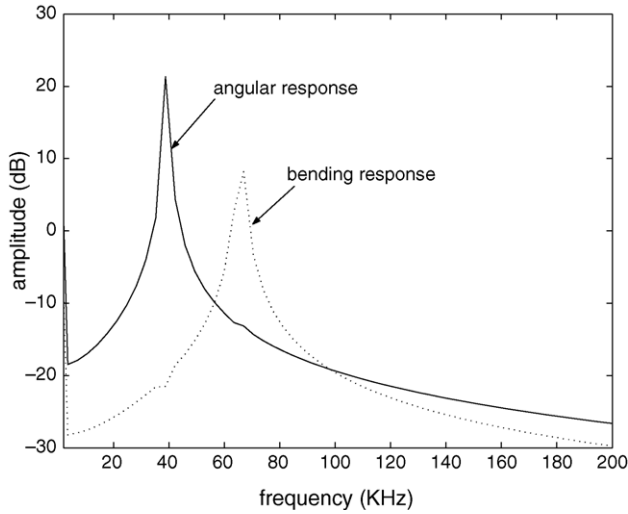
$$(27)$$

Figure 7. Stable equilibrium angle versus η (color figure available online).

Now, the homotopy form is constructed as follows.

$$\Im(\Theta, \eta, \lambda, P) = L(\Theta, \eta, \lambda) + P.N(\Theta, \eta, \lambda) = 0 \tag{28}$$

In equation (28), $\Im(\Theta, \eta, \lambda, P)$ is the homotopy form and P is an embedding parameter which serves as perturbation parameter. When $P = 1$, the homotopy form would be the same as the equilibrium equation and when $P = 0$, homotopy form would be the linear part of equilibrium equation. The value of the dimensionless rotation angle Θ can also be expanded in terms of the embedded parameter P as follows.

$$\Theta = \Theta_0 + P\Theta_1 + P^2\Theta_2 + P^3\Theta_3 + \cdots \tag{29}$$

Substituting equation (29) into homotopy form yields:

$$\Im(\Theta, \eta, \lambda, P) = L\big(\Theta_0 + P\Theta_1 + P^2\Theta_2 + \ldots, \eta, \lambda\big)$$
$$+ P \cdot N\big(\Theta_0 + P\Theta_1 + P^2\Theta_2 + \ldots, \eta, \lambda\big) = 0 \tag{30}$$

The Taylor series expansion of right hand side of equation (30) in terms of P would be as

$$\Im(\Theta, \lambda, P) = L(\Theta_0, \eta, \lambda) + \left(\Theta_1 \frac{\partial L(\Theta_0, \eta, \lambda)}{\partial \Theta_0} + N(\Theta_0, \eta, \lambda)\right) P$$
$$+ \left(\Theta_2 \frac{\partial L(\Theta_0, \eta, \lambda)}{\partial \Theta_0} + \Theta_1 \frac{\partial N(\Theta_0, \eta, \lambda)}{\partial \Theta_0}\right) P^2$$
$$+ \left(\Theta_3 \frac{\partial L(\Theta_0, \eta, \lambda)}{\partial \Theta_0} + \Theta_2 \frac{\partial N(\Theta_0, \eta, \lambda)}{\partial \Theta_0} + \frac{1}{2}\Theta_1^2 \frac{\partial^2 N(\Theta_0, \eta, \lambda)}{\partial \Theta_0^2}\right) P^3$$
$$+ \cdots = 0 \tag{31}$$

Since the homotopy form must be unified with zero, the coefficients of all powers of P must be zero. This, leads to the following equations.

$$L(\Theta_0, \eta, \lambda) = 0 \tag{32}$$

$$\Theta_1 \frac{\partial L(\Theta_0, \eta, \lambda)}{\partial \Theta_0} + N(\Theta_0, \eta, \lambda) = 0 \tag{33}$$

$$\Theta_2 \frac{\partial L(\Theta_0, \eta, \lambda)}{\partial \Theta_0} + \Theta_1 \frac{\partial N(\Theta_0, \eta, \lambda)}{\partial \Theta_0} = 0 \tag{34}$$

$$\Theta_3 \frac{\partial L(\Theta_0, \eta, \lambda)}{\partial \Theta_0} + \Theta_2 \frac{\partial N(\Theta_0, \eta, \lambda)}{\partial \Theta_0} + \frac{1}{2}\Theta_1^2 \frac{\partial^2 N(\Theta_0, \eta, \lambda)}{\partial \Theta_0^2} = 0 \tag{35}$$
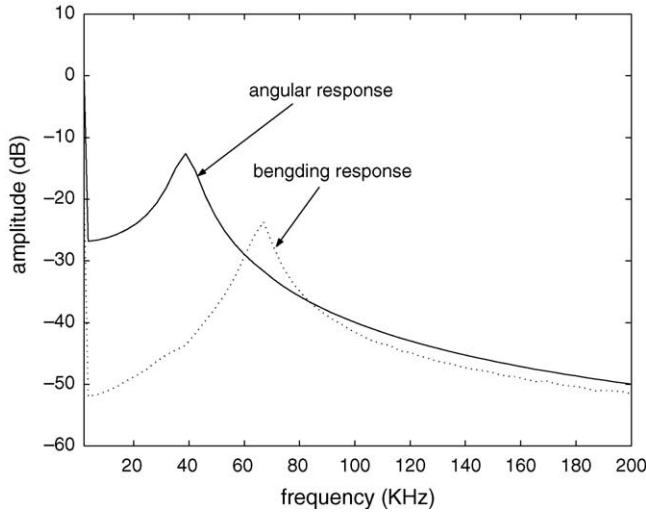
Figure 8. Estimation of nano/micromirror's rotation angle using HPM (color figure available online).

With solving equations (32) to (35), the parameters $\Theta_i \; 0 \leq i \leq 3$ are found as follows.

$$\Theta_0 = \frac{3(\eta + \lambda)}{2(3 - \eta - 4\lambda)} \tag{36}$$

$$\Theta_1 = -N(\Theta_0, \eta, \lambda) \bigg/ \left(\frac{\partial L(\Theta_0, \eta, \lambda)}{\partial \Theta_0} \right) \tag{37}$$

$$\Theta_2 = -\Theta_1 \left(\frac{\partial N(\Theta_0, \eta, \lambda)}{\partial \Theta_0} \right) \bigg/ \left(\frac{\partial L(\Theta_0, \eta, \lambda)}{\partial \Theta_0} \right) \tag{38}$$

$$\Theta_3 = -\left(\Theta_2 \frac{\partial N(\Theta_0, \eta, \lambda)}{\partial \Theta_0} + \frac{1}{2} \Theta_1^2 \frac{\partial^2 N(\Theta_0, \eta, \lambda)}{\partial \Theta_0^2} \right) \bigg/ \left(\frac{\partial L(\Theta_0, \eta, \lambda)}{\partial \Theta_0} \right) \tag{39}$$

The value of Θ can be found by substituting $\Theta_i \; 0 \leq i \leq 3$ and $P = 1$ in equation (29). In Figure 8 the results of the numerical simulations is compared with those of analytical HPM results for the special case of $\lambda = 0.1$. It is observed that HPM closely approximates the rotation angle of the mirror. Obviously increasing the order of perturbation approximation would lead to more precise results, but increasing the order of the perturbation approximation more than 6 will not improve the accuracy of the obtained response significantly. As a result, a sixth order perturbation approximation used in HPM can precisely predict the nano/micromirror behaviour under the combined effects of capillary and Casimir force.

4. CONCLUSION

The dimensionless equilibrium equation of the nano/micromirror under capillary force was obtained considering Casimir force. The dependency of the critical

tilting angle on the instability numbers defined in the article was investigated. Results show that neglecting the Casimir effect on the static equilibrium of nano/micromirrors under capillary force may lead to considerable error in predicting stability limits of the mirror and can lead to an unstable design.

It was observed that rotation angle of the mirror due to capillary force highly depends on the Casimir effect applied to the mirror. HPM was utilized to analytically predict the rotation angle and stability limits of the nano/micromirrors. It was found that a sixth order perturbation approximation can accurately estimate the rotation angle of the mirror due to capillary and Casimir loading. The presented results in this article can be used for stable design and fabrication of nano/micromirrors using wet etching process where the gap between the mirror and the underneath substrate is less than a few micrometers and as a result, both capillary and Casimir forces have significant effects on the system.

REFERENCES

Abdel-Rahman, Eihab M. and Ali H. Nayfeh. 2003. Secondary resonances of electrically actuated resonant microsensors. *Journal of Micromechanics and Microengineering* 13 (3): 491–501.

Bai, Yanhui, John Tze Wei Yeow, and Brian Wilson. 2007. A characteristic study of micromirror with sidewall electrodes. *International Journal of Optomechatronics* 1 (3): 1323–1328.

Bordag, Michael, Umar Mohideen, and Vladimir Mostepanenko. 2001. New developments in the Casimir effect. *Physics Report* 353: 1–205.

Chao, P. C. P., Cheng Chiu, and Chieh Tsai. 2006. A novel method to predict the pull in voltage in a closed form for micro-plates actuated by a distributed electrostatic force. *Journal of Micromechanics and Microengineering* 16 (5): 986–998.

Dickensheets, David and Gordon Kino. 1998. Silicon-micromachined scanning confocal optical microscope. *Journal of Microelectromechanical Systems* 7 (1): 38–47.

Ford, Joseph, Vladimir Aksyuk, David Bishop, and James Walker. 1999. Wavelenghth add-drop swiching using tilting micromirrors. *Journal of Lightwave Technology* 17 (5): 904–911.

Fortes, Manuel. 1982. Axisymmetric liquid bridges between parallel plates. *Journal of Colloid and Interface Science* 88 (2): 338–352.

Gambhir, Murary. 2004. *Stability Analysis and Design of Structures*. Berlin: Springer.

Guo, Jian and Yapu Zhao. 2004. Influence of van der Waals and Casimir forces on electrostatic torsional actuators. *Journal of Microelectromechanical Systems* 13 (6): 1027–1035.

Guo, Jian, Li Zhou, and Yapu Zhao. 2009. Instability analysis of torsional MEMS/NEMS actuators under capillary force. *Journal of Colloid and Interface Science* 331 (2): 458–462.

Gusso, Andre and Guilherme Delben. 2007. Influence of the Casimir force on the pull-in parameters of silicon based electrostatic torsional actuators. *Sensors and Actuators A* 135 (2): 792–800.

He, Jihuan. 2000. A coupling method of a homotopy technique and a perturbation technique for non-linear problems. *International Journal of Non-Linear Mechanics* 35 (1): 37–43.

Hornbeck, Larry. 1991. Spatial light modulator and method. US Patent: 5,061,049.

Huang, Jian, A. Q. Liu, Z. L. Deng, Q. X. Zhang, J. Ahn, A. Asundi. 2004. An approach to the coupling effect between torsion and bending for electrostatic torsional micromirrors. *Sensors and Actuators A* 115 (1): 159–167.

Jang, Joonkyung, George Schatz, and Mark Ratner. 2004. Capillary force in atomic force microscopy. *Journal of Chemical Physics* 120 (3): 1157–1160.

Knospe, Carl and Ali Nezamoddini. 2009. Capillary force actuation. *Journal of Micro-Nano Mechatronics* 5 (3): 57–68.

Lin, Wen and Yapu Zhao. 2005a. Casimir effect on the pull-in parameters of nanometer switches. *Microsystem Technologies* 11 (2–3): 80–85.

Lin, Wen and Yapu Zhao. 2005b. Nonlinear behavior for nanoscale electrostatic actuators with Casimir force. *Chaos, Solitons and Fractals* 23 (5): 1777–1785.

Li, Xide and Yun Peng. 2006. Investigation of capillary adhesion between the microcantilever and the substrate with electronic speckle pattern interferometry. *Applied Physics Letters* 89: 234104.

Liu, Haipeng, Shiqiao Gao, Shaohua Niu, and Lei Jin. 2010. Analysis on the adhesion of micro-comb structure in MEMS. *International Journal of Applied Electromagnetics and Mechanics* 33 (3–4): 979–984.

Maluf, Nadim and Kirt Williams. 1999. *An Introduction to Microelectromechanical Systems Engineering. Second Edition*, MicroelectromechanicalSystems (MEMS) Series. Boston, London: Artech House Inc.

Mastrangelo, Carlos and C. H. Hsu. 1993. Mechanical stability and adhesion of microstructures under capillary forces-part 1: Basic theory. *Journal of Microelectromechanical Systems* 2 (1): 33–43.

Mastrangelo, Carlos and C. H. Hsu. 1993. Mechanical stability and adhesion of microstructures under capillary forces-part 2: Experiments. *Journal of Microelectromechanical Systems* 2 (1): 44–55.

Moeenfard, Hamid, Mohammad Kahrobaiyan, and Mohammad Ahmadian. 2010. Application of the extended Kantorovich method to the static deflection of microplates under capillary force. ASME International Mechanical Engineering Congress and Exposition, IMECE2010:39517.

Moeenfard, Hamid, Mahdi Mojahedi, and Mohammad Ahmadian. 2011. A homotopy perturbation analysis of nonlinear free vibration of timoshenko microbeams. *Journal of Mechanical Science and Technology* 25 (3): 279–285.

Mojahedi, Mahdi, Hamid Moeenfard, and Mohammad Ahmadian. 2009. A new efficient approach for modeling and simulation of nano- switches under combined effects of intermolecular surface forces and electrostatic actuation. *International Journal of Applied Mechanics* 1 (2): 349–365.

Mojahedi, Mehdi, Hamid Moeenfard, and Mohammad Ahmadian. 2010. Analytical solutions for the static instability of nano-switches under the effect of Casimir force and electrostatic actuation. ASME International Mechanical Engineering Congress and Exposition, 63–69.

Ramezani, Asghar, Aria Alasty, and Javad Akbari. 2007. Pull-in parameters of cantilever type nanomechanical switches in presence of Casimir force. *Nonlinear Analysis: Hybrid Systems* 1 (3): 364–382.

Ramezani, Asghar, Aria Alasty, and Javad Akbari. 2008. Analytical investigation and numerical verification of Casimir effect on electrostatic nanocantilevers. *Microsyst Technol* 14 (2): 145–157.

Rao, Sinjiresu. 2007. *Vibration of Continuous Systems*. New Jersey: John Wiley & Sons.

Serry, Michael, Dirk Walliser, and Jordan Maclay. 1998. The role of the Casimir effect in the static deflection and stiction of membrane strips in microelectromechanical systems (MEMS). *Journal of Applied Physics* 84 (5): 2501–2506.

Sirvent, Raul, Ovando Palomino, and Gregorio Cocoletzi. 2009. Pull-in control due to Casimir forces using external magnetic fields. *Applied Physics Letters* 95 (5): 051909.

Tahami, Farid, Hamed Mobki, Ali Janbahan, and Ghader Rezazadeh. 2009. Pull-in phenomena and dynamic response of a capacitive nano-beam switch. *Sensors & Transducers Journal* 110 (11): 26–37.